UNITED NATIONS UNIVERSITY
GEOTHERMAL TRAINING PROGRAMME
Orkustofnun, Grensásvegur 9,
IS-108 Reykjavík, Iceland

Reports 2007
Number 23

MONITORING OF MICROEARTHQUAKES AND ACOUSTIC EMISSIONS WITHIN THE HENGILL-HELLISHEIDI GEOTHERMAL RESERVOIRS, JUNE-AUGUST 2007

Anastasia W. Wanjohi
University of Nairobi
School of Physical and Biological Sciences, Department of Geology
P.O.Box 30197- 00100, Nairobi
KENYA
immaculateann@yahoo.com

ABSTRACT

With increased emphasis on geothermal development, new exploration methods are needed in order to improve the general understanding of geothermal reservoirs, characterize their extent and assess the potential for sustainable utilization. Monitoring of microearthquakes and acoustic emissions within geothermal areas may provide a new tool for evaluating the spatial extent of geothermal fields, their dynamics and model rock-fluid interactions. In this project, data was collected within the Hengill-Hellisheidi geothermal area. A temporary seismic network was in operation from June 13 to August 13, 2007 and the area covered was 220km^2**.** In this period more than 60 events were recorded during the field campaign, which were located using the program Hypoinverse 2000.

Seismicity in the Hengill-Hellisheidi area during the observation period was low. Most of the events followed a NW-SE trend, from Reykjadalur, across Ölkelduháls into Hengill, correlating with surface geothermal manifestations. A few events were also located within the fissure swarm north and south of Hengill. Earthquakes at Ölkelduháls clustered at 4-6 km depth whereas events within the Hengill fissure swarm have a broader depth range, from 0 to 9 km. These earthquakes are most likely associated with tectonic movements or hydraulic fracturing and fluid flow within the geothermal systems.

A preliminary study of the noise distribution within the Hengill-Hellisheidi geothermal fields has revealed 4-6 Hz spectral peaks at seismic stations located in the vicinity of surface geothermal manifestations. Further investigation is needed to determine their relationship to the Hengill-Hellisheidi geothermal field. Spectral peaks within the range of 8-30 Hz have been observed at most of the stations and are probably related to various sources of noise such as wind and overpressurized boreholes.

1. INTRODUCTION

Geophysical exploration is the study of the Earth‘s physical parameters and its surroundings using physical methods such as seismic, electrical and electromagnetic, magnetic and radioactivity methods.

It plays an important role in exploring for geothermal resources, in delineating, evaluating and monitoring utilization of geothermal fields. Temperature measurements and electrical/electromagnetic methods detect anomalous temperatures and conductivity anomalies which are coupled to geothermal activity. They are widely used in siting drilling targets (Telford et al., 1990). Seismic methods have not been so popular in geothermal exploration but in the last decade or so, their importance has been recognised. More than a dozen countries are involved in utilizing geothermal resources, both moderate- and high-temperature geothermal systems for generating electric power, and lower temperature resources of several types for space heating and industrial processing (Fridleifsson and Freeston, 1994).

The basic components of a geothermal system are: a heat source, a reservoir, and conduits or pathways to allow circulation of fluid. Where impermeable cap rock is present the geothermal system can be pressurised (Figure 1). The practical objective of geothermal research is to locate potentially attractive geothermal fields that can be exploited for electric power generation and other uses. Heat sources, availability and characteristics of fluids, reservoir temperature and flow channels are the main parameters investigated. They are sometimes manifested at the surface whereas in other cases there are virtually no surface expressions of an underlying resource. To evaluate these 'blind resources', different geological, geochemical and geophysical methods have been applied.

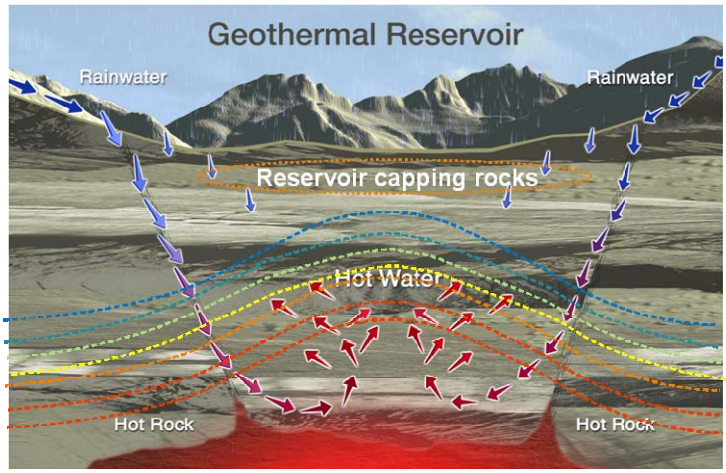

FIGURE 1: Geothermal system showing its components; differently shaded/coloured dotted lines show different temperatures as the water heats up (Geothermal Education Office, 2007)

Seismic methods use the propagation of elastic waves to image sources and structures within the Earth. Earthquake locations and fault plane solutions give information about active faults and permeable zones in a geothermal system. In the geothermal industry, monitoring of seismic activity has been used to study geothermal reservoirs and their processes. These processes can be ground noise (microseismics) generated by the geothermal system (e.g. boiling and/or convective flow), microearthquakes and earthquakes on active faults, and hydraulic fracturing and tensile cracking of cooling intrusions (Hersir and Björnsson, 1991). Earthquakes are an essential part of geothermal systems for they break up the bedrock by faulting and fissuring and provide paths for water to percolate down into the thermal areas creating permeability, thus, geothermal areas are constantly changing (Bolt, 2004). Many geothermal systems exist in volcano-tectonic areas and are characterized by a high level of microseismic activity. Numerous studies show that recent intrusions are associated with high levels of earthquake activity and tectonic activity can thus indicate cooling intrusions.

The main objective of this study was to give the author practical training in geothermal exploration using seismic methods, emphasizing seismic data interpretation and analysis of naturally occurring local seismicity. To achieve this, highly precise earthquake locations are needed as well as a dense coverage of seismic stations. The locating of earthquakes in the geothermal area was done using a temporary seismic network (HH2007). The results were compared with that of the automatic SIL network and used to understand better the Hengill-Hellisheidi seismicity in relation to the geothermal fields. A pilot spectral analysis of the regional "seismic noise" was also performed.

2. BACKGROUND

2.1 The Hengill volcanic system

2.1.1 Tectonic setting

The Hengill central volcano is characterised by tensional stress parallel to the N110°E spreading direction (Sigmundsson et al., 1997). The volcano is intersected by a fracture system or fissure swarm that extends for 60-80 km from southwest to northeast. There are also strike-slip faults in a N-S direction. The fracture network is periodically activated providing conduits for the episodic eruption of basalt and the emplacement of dykes and also controls the circulation of hot water and steam from the centre of the Hengill system. Besides the major fissure swarm, there are some faults and eruptive fissures transecting the centre of Hengill in a NW-SE direction towards the Hveragerdi system, i.e. perpendicular to the main tectonic trend. The Hengill volcanic complex is suggested to be divided into the Hveragerdi-Grensdalur (Graendalur) volcanic system (eastern part of the area) that was active between 700,000 and 30,000 years ago, but is now partially eroded down to the chlorite zone; the Hrómundartindur system, whose surface formations are younger than 0.2 Ma; and the currently active Hengill system (Saemundsson and Fridleifsson, 1980). The magma moves into the shallow crust at temperatures of about 1200°C and supplies heat to the hydrothermal system (Bödvarsson et al., 1990).

2.1.2 Geology and geothermal activity

Iceland is a relatively young country built up over the past 16 Ma by basaltic volcanism along the slow-spreading Mid-Atlantic ridge. It is located at the junction of the Mid-Atlantic ridge and the Greenland-Iceland-Faeroe ridge (Figure 2), the former being part of the global mid-oceanic ridge system that defines the constructive plate boundary between the American and the Eurasian plates. The spreading rate is close to 2 cm/year (DeMetz et al., 1994).

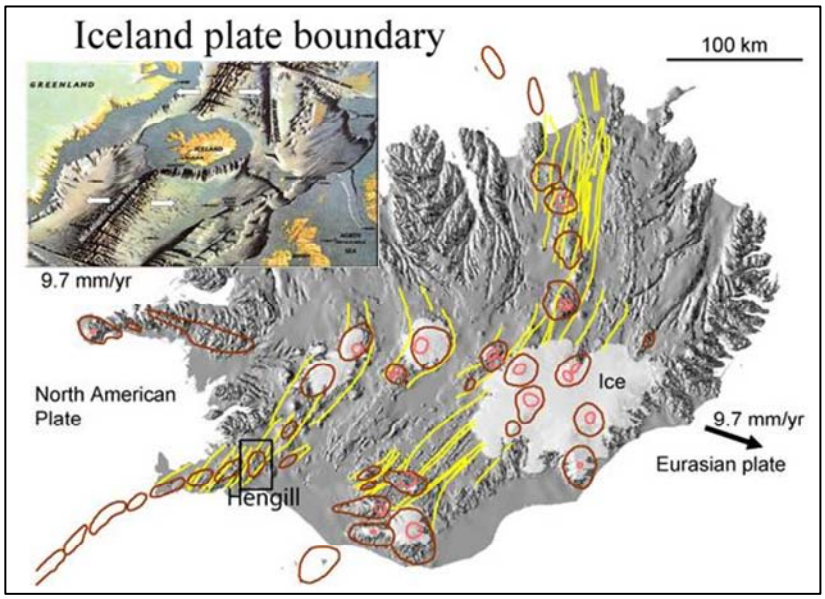

FIGURE 2: Regional map of Iceland showing the study area (black square); inset is a map showing Iceland in relation to the Mid-Atlantic ridge (mod. from Einarsson and Saemundsson, 1987)

The structure and the activity of Iceland‘s plate boundary is strongly influenced by the Icelandic plume (Tryggvason et al., 1983) and expressed by a series of seismic and volcanic zones. It comprises four presently active volcanic zones: Northern Volcanic Zone (NVRZ), Eastern Volcanic Zone (EVRZ), the Western Volcanic Zone (WVRZ) and the Reykjanes Peninsula (RP). The South Iceland Seismic Zone (SISZ) is a transform zone between WVRZ and EVRZ characterised by high seismic activity (Stefánsson et al., 1993). Each rift zone is made up of volcanic systems, consisting of a central volcano transected by a fissure swarm (Figure 2). Some central volcanoes have developed calderas (Saemundsson, 1978).

Located at the triple junction of the RP, WVZ and SISZ, (Saemundsson, 1979), the Hengill-Hrómundartindur-Grensdalur volcanic systems sustain powerful geothermal fields with an areal extent

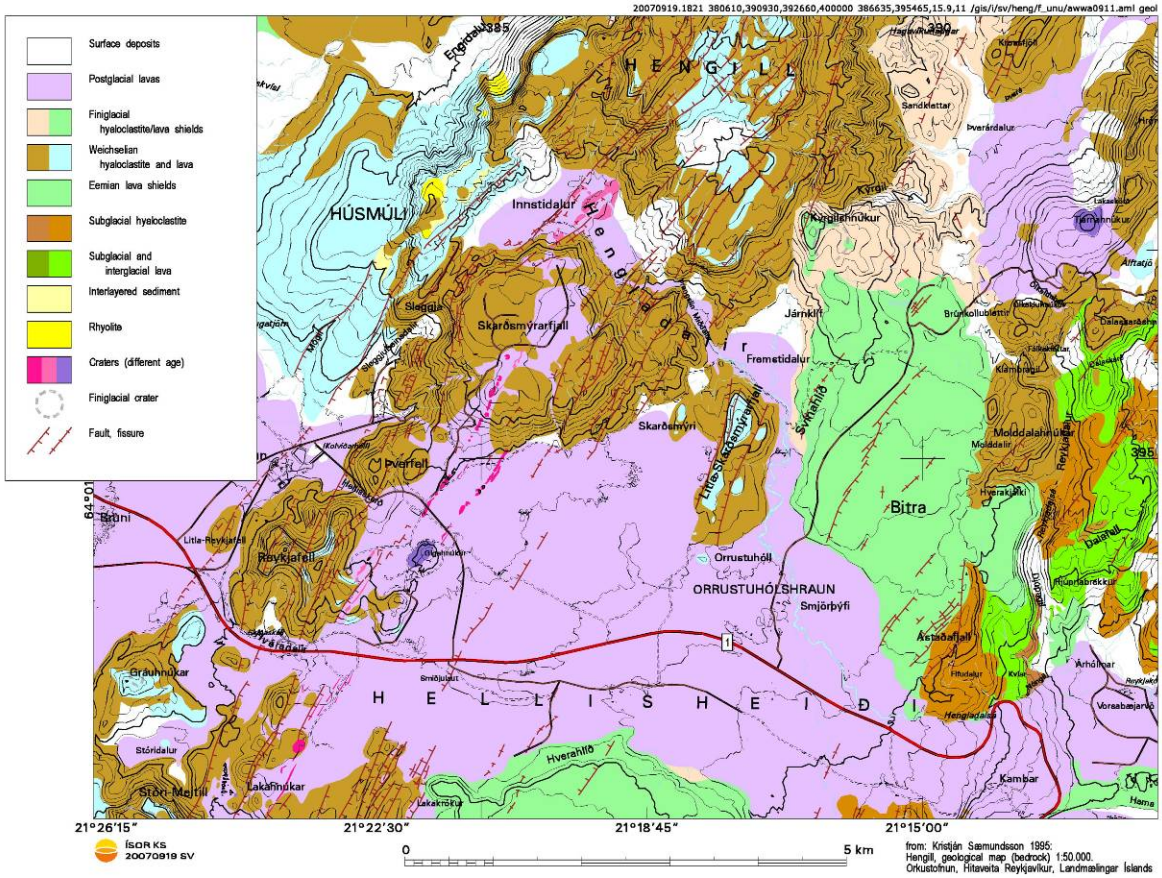

FIGURE 3: Detailed geological map of the area (Saemundsson, 1995a)

of 50 km^2. The Hengill central volcano, formed in the past 0.8 Ma, is the site of powerful geothermal fields with an areal extent of 50 km^2. At least three volcanic eruptions have occurred in the area in the last 11,000 years; the most recent one 2,000 years ago (Saemundsson, 1995a, b). Bedrock types in the area are volcanic, mainly composed of various lithofacies of subglacially formed hyaloclastites (basaltic breccias, tuffs and pillow lava) and Holocene lava flows (Figure 3).

The geothermal activity is related to recent northeast-trending dykes and faults within the Hengill fissure swarm, from Hellisheidi to Nesjavellir, north of Hengill (Árnason, 1993). Surface geothermal activity is also present within the older volcanic systems (Figure 4), Hrómundartindur and Grensdalur, further east, following a northwest striking trend from Hengill across Ölkelduháls to Klambragil, Reykjadalur and Grensdalur-Hveragerdi (Figure 4). During enhanced earthquake activity, changes have been observed in the surface geothermal activity (Sigmundsson et al., 1997; Clifton et al., 2002). Investigation of the Hengill volcanic complex indicates that super critical conditions probably exist at a shallow depth (5 km) and perhaps at less than 3 km depth associated with the youngest volcanic structures in the western part of the Nesjavellir system (Fridleifsson et al., 2003). The Hengill-Hellisheidi geothermal system is active, and is estimated to have a power potential of 1 GW of electricity (Reykjavík Energy, 2007).

2.2 Hengill-Hellisheidi: Seismic activity and crustal structure

Present day seismicity in Iceland is governed by tectonic complexities that derive from the westward motion of the Mid-Atlantic ridge relative to the Icelandic hot spot (Saemundsson, 1978). Most earthquakes in Iceland are of the usual high frequency type, reflecting brittle crust, though lower frequency earthquakes also occur, especially in volcanic regions (Einarsson and Brandsdóttir, 2000). Most destructive earthquakes in Iceland in historical times, have originated within the SISZ, most

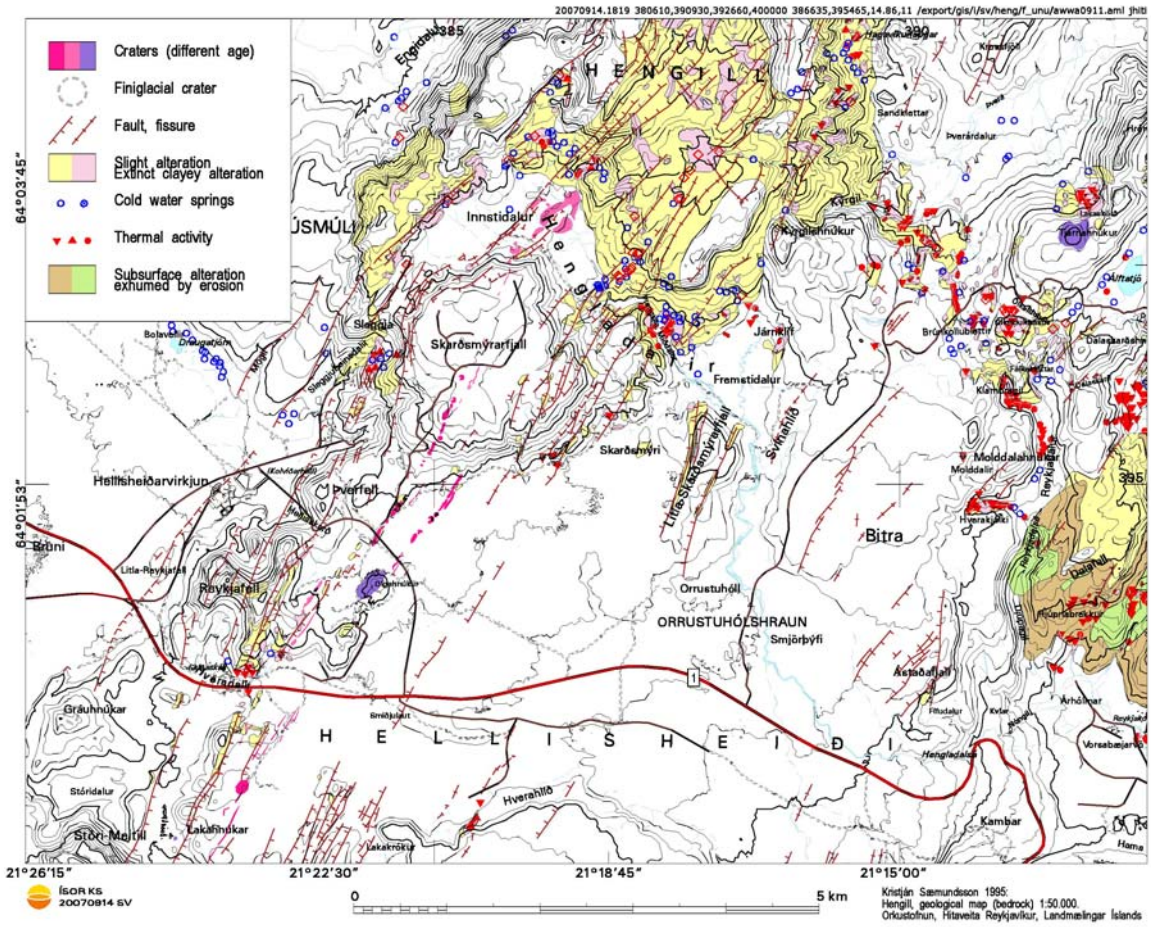

FIGURE 4: Geothermal activity, alteration and major tectonic features of the study area (Saemundsson, 1995b)

recently in 2000. (Einarsson, 1991; Jakobsdóttir et al., 2002; Clifton and Einarsson, 2005; Hackman et al., 1990, Sigmundsson et al., 1997). Current seismicity of the SISZ is characterised by semi-continuous clustering activity and aftershocks from the June 2000 earthquakes (Jakobsdóttir at al., 2002). Background seismicity throughout the Hengill triple junction consists of continuous, small magnitude earthquakes (Foulger and Einarsson, 1980; Foulger, 1988a; Sigmundsson et al., 1997; Ágústsson and Halldórsson, 2005).

Between 1994 and 1998, the Hengill triple junction was subjected to both tectonic extension and shear during episodic periods of enhanced seismicity related to strike-slip and normal faulting (Clifton et al., 2002), culminating in a ML=5.1 earthquake on June 4, 1998 and a ML=5 earthquake on November 13, 1998. More than 80,000 earthquakes were located within the Hengill, Hrómundartindur and Grensdalur volcanic systems during this period. Geodetic measurements, GPS, surface levelling and InSAR detected maximum uplift of 2 cm/yr above a modelled inflation centre at 6.5-7 km depth south of Ölkelduháls, between the Hrómundartindur and Grensdalur volcanic systems (Sigmundsson et al., 1997; Feigl et al., 2000). A number of surface fault movements on segmented right-lateral strike-slip faults were detected in association with the June 4th event (Feigl et al., 2000; Clifton et al., 2002).

2.3 Synthesis of previous work

The local earthquake tomographic (LET) study of the Hengill volcanic area by Foulger and Toomey, (1989) and Toomey and Foulger (1989) revealed high-velocity bodies within the Grensdalur and Hrómundartindur volcanic centres, interpreted as hot, but solidified, intrusions, presently fuelling

surface geothermal areas within these systems. A small low-velocity body (approximately 3 km^3) imaged beneath the northeast flank of the Hengill central volcano was tentatively interpreted as a region containing partial melt.

A revised three-dimensional crustal model using a digital seismic network deployed in 1991 (Miller et al., 1998) was unable to confirm the existence of a low-velocity body beneath NE-Hengill, suggesting it to be an artefact of the inversion procedure and showing Hengill to be devoid of major compressional velocity anomalies. However, Tryggvason et al. (2002), also using LET, imaged reduced P- and S-velocities beneath the Hengill fissure swarm with velocities ranging from 5.9–6.3 km/s and 3.4–3.65 km/s at 3–9 km depth and a Vp/Vs-ratio below 1.7, which they attributed to a high-porosity region containing supercritical fluids.

Miller et al. (1998) constrained a ~40 km^3 high-velocity body of > 0.4 km/s at 1-5 km depth beneath the Grensdalur volcanic centre and a ~20 km^3 body of > 0.3 km/s at 2-5 km depth underlying Ölkelduháls. The third high-velocity body extends down to 4 km depth beneath Húsmúli, an old basalt shield on the southwest flank of Hengill. Similarly, Tryggvason et al. (2002) imaged high velocities beneath Hrómundartindur, Húsmúli, and Grensdalur, although at slightly greater depths. No S-wave attenuation, indicative of areas of partial melt, has been observed within the Hengill region (Miller et al., 1998; Tryggvason et al., 2002). However, the LET models do not rule out the possible presence of small pockets of melt (0.01 km^3) as suggested by Sigmundsson et al. (1997) at 6.5 km depth beneath the Hrómundartindur volcano.

Negative Vp/Vs anomalies imaged within many geothermal areas have been attributed to variations in rock compressibility, i.e. variations in porosity and pore-fluid pressure caused by variations in temperature or the presence of vapour. A NW-SE trending anomaly of low Vp/Vs was also observed from Grensdalur, across Ölkelduháls to the region south of Nesjavellir, extending from the surface to ~4 km depth (Miller et al., 1998). This low Vp/Vs anomaly is dominated by two vertical zones, dipping southeast from S-Nesjavellir and northwest from Grensdalur. The deeper parts of the low Vp/Vs bodies correlate with high Vp volumes. Whereas the deepest parts of the high Vp bodies are seismogenic, the low Vp/Vs bodies are nearly aseismic. Using LET and active sources, Tryggvason et al. (2002) observed Vp/Vs ratios generally below 1.7 at 3-4 km depth.

Refraction and LET studies show the thickness of the upper crust (depth to the iso-velocity contour of 6.5 km/s) to be close to 7 km beneath the Hengill system whereas the overall crustal thickness ranges from 17 to 20 km within this region (Bjarnason et al., 1993; Weir et al., 2001; Tryggvason et al., 2002).

Non-double couple focal mechanisms, initially observed at Hengill by Foulger (1988b), have been attributed to the process of contraction cracking within the cooling geothermal heat source (implosions) or tensile opening of cracks (explosions). Their distribution has been used to demarcate hot rocks fuelling the geothermal reservoir. Initial focal mechanisms indicated that about half of the Hengill events exhibit normal and strike-slip faulting in response to a horizontal, NW-oriented minimum compressive stress, while the other half shows evidence for mechanisms with a non-double couple component. However, Miller et al. (1998) concluded that 75% of the earthquakes recorded by the 1991 Hengill seismic network had a non-double-couple (non-DC) mechanism, whereas 25% were consistent with a double-couple mechanism. The non-DC mechanisms were observed to be consistent with simultaneous tensile and shear faulting, the dominant mode of shear faulting being right lateral on north-northeast-sticking near-vertical faults.

Björnsson et al. (1986) conducted a regional geophysical survey in the Hengill area observing that the continuous micro-earthquake activity within the region can be correlated with surface geothermal activity. In the absence of an extended magma chamber in the upper crust beneath Hengill, they considered the geothermal system to be fed from deep circulation (to about 5 km) of groundwater in a highly fractured crust with a surface temperature gradient of 150°C/km.

3. SEISMIC WAVES AND BASIC THEORY

3.1 Types of seismic waves

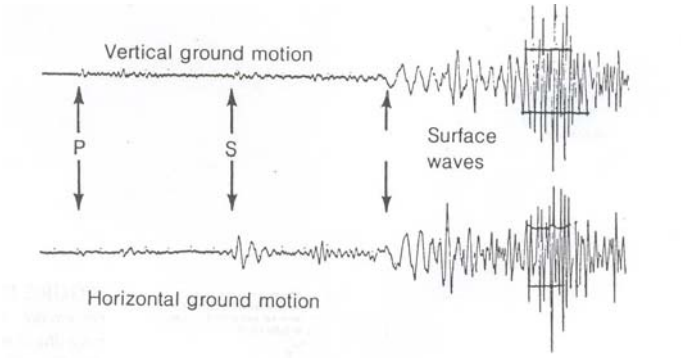

FIGURE 5: Seismogram showing P-waves, S-waves and surface waves (taken from Press and Siever, 1974)

Seismic waves are caused by the sudden breaking of rock within the earth or by an explosion. They travel through the earth and are recorded on seismographs (when stress varies with time, strain varies similarly and the balance between stress and strain results in seismic waves). The waves travel at velocities that depend on the elastic moduli and are governed by equations of motion (Lay and Wallace, 1995). The waves are refracted and reflected at velocity discontinuities in the crust. There are different kinds of seismic waves which travel in different ways across the earth. The two main types of waves are body waves and surface waves (Figure 5). Body waves can travel through the earth's interior, but surface waves can only move along the surface of the planet like ripples on water. Earthquakes radiate seismic energy as both body and surface waves.

Body waves travel through the interior of the earth and have shorter travel times than surface waves. There are two kinds of body waves: primary (P-waves) and secondary (S-waves). The velocity of both P and S-waves are dependent on density and elastic moduli.

Primary or compressional waves (P-waves) are the first waves to arrive at a seismic station and are faster than S-waves. They can move through solid rock and liquid by pushing and pulling the material they move through just like sound waves push and pull the air. P wave particles move in the same direction that the wave is moving in, the direction that the energy is travelling in, which is called the direction of wave propagation. The polarization of P-waves is always longitudinal (in isotropic and homogeneous solids). This means that the particles in the body of the earth have vibrations along or parallel to the direction of travel of the wave energy.

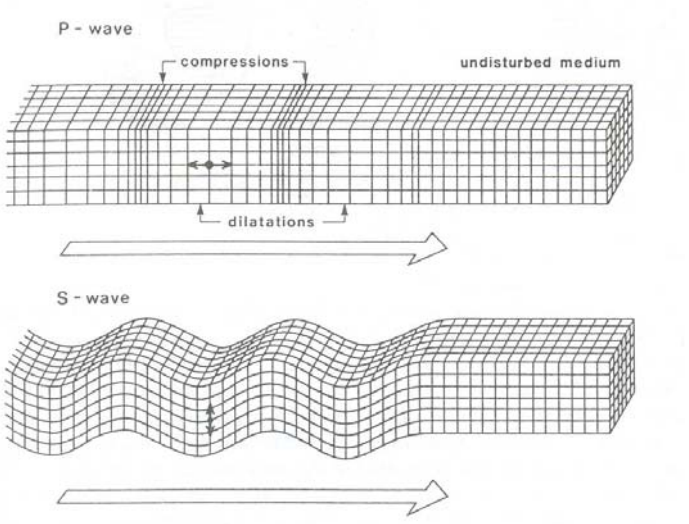

FIGURE 6: P- and S-waves travelling through a medium; the large arrows show direction of propagation and the small arrows show the particle motion

Secondary waves (S-waves) are transverse waves, which make the earth shake from side to side (pure shear strain). Slower than P-waves, they arrive second and can only move through solid and not through liquid media. It is this property of S-waves that led seismologists to conclude that the Earth's outer core is a liquid. These waves are, therefore, strongly attenuated or disappear completely when they travel through partially molten rocks. S-waves move rock particles up and down or side-to-side, perpendicular to the direction of wave propagation (Figure 6).

3.2 Earthquake location

Earthquakes give information on the stress field and the tectonic nature of the area where they occur and on the transmission path from source to receiver by observation of seismic waves. The location of earthquakes is determined from the time taken by P and S-waves to travel from the focus to a seismograph. The travel time of a seismic wave (e.g. P and S) from a source to a given point on Earth´s surface (seismograph) depends on the distance between the two points (Bolt, 2004). To determine the location of an earthquake, **m** = (t,x,y,z), we measure the arrival of seismic waves at seismic stations assuming knowledge of the velocity structure between the hypocenter and the seismic station.

The travel time to a station from any seismic event can be defined by a non-linear function, *G*:

$$T_{obs} = G(\mathbf{m};\mathbf{u}),$$

where T_{obs} = Arrival time measured at a seismic station;
m = (t,x,y,z) is the origin time and geographical coordinates of the hypocenter, and
u = Velocity model used.

For a homogeneous earth with velocity *V*, the *i*-th observed arrival time can be written as:

$$T_i = t_0 + [(x_i-x)^2 + (y_i-y)^2 + (z_i-z)^2]^{1/2}/V \qquad (i = 1,2,3.....,N)$$

where $\boldsymbol{x}_i$ = (x_i,y_i,z_i) = The location of the *i*-th station;
t_0 = The common time origin;
x = (x,y,z) = The event location; and
N = Number of observations.

This is already non-linear in the event location coordinates. If the velocity is variable in space, further non-linearity is introduced through the dependence of ray paths on velocity.

To proceed, this non-linear problem can be linearized and solved through a series of iterations. This is done by expanding the function *G* using the Taylor series around a starting model, $\mathbf{m}_0$. We try to find a better solution by perturbing the model until some convergence criteria are reached. The quality of the solution will depend strongly on these initial estimates as the problem is being solved iteratively (Menke, 1984):

$$T_i = G_i(\mathbf{m}_0;\mathbf{u}) + \nabla G_i|m = m_0\,(\delta\mathbf{m},\mathbf{u}) + \ldots\ldots\ldots\ smaller\ terms$$

where ∇G is an $N\times4$ matrix with the *i*-th row defined as:

$$\nabla G_i = (\partial T_i/\partial t,\partial T_i/\partial x,\partial T_i/\partial y,\partial T_i/\partial z)\ evaluated\ at\ (t,x,y,z) = (t_0,x_0,y_0,z_0).\mathbf{m} = \mathbf{m} - \mathbf{m}_0$$

Here the model perturbation, $\delta\mathbf{m}$, is referenced to the model from the previous iteration, $\mathbf{m_0}$. This is a linear relationship between **m** and **T**, which we can reorganize in a matrix form by defining a data vector, **d**:

$$d_i = T_i - G_i(\mathbf{m}_0;\mathbf{u}),\ \text{(observed minus calculated time)}$$

Each iteration can thus be expressed as a linear inverse problem of the form:

$$\mathbf{d} = \mathbf{G}\delta\mathbf{m},$$

where **G** contains the derivatives $\nabla G_i|_{\mathbf{m}=\mathbf{m}_0}$.

This is then solved by a standard linear equation solver, e.g. the Gauss-Newton method or damped least squares. Detailed mathematical formulation of the non-linear earthquake-location problem is discussed by e.g. Lee and Stewart (1981) and Lay and Wallace (1995).

The difference (misfit) between observed and calculated arrival times, which is determined from the model of the previous iteration, is the residual arrival time on each seismic station for a given event. This residual is minimised in a least-squares sense by iteration where the location of the hypocenter is changed. In standard earthquake-location procedures like Hypoinverse (Klein, 2000), the velocity model is fixed and therefore the location is the only unknown. Both P and S-wave picks can be used to determine hypocenter locations. The program requires the user to have a velocity model for both wave types, a station list, an initial location and phase data input files. The location method involves the following steps:

- Calculating the root-mean-square residual time for the current location, σ_T;
- Calculating an adjustment vector, $\delta\mathbf{m}$, in the direction which minimises the σ_T;
- Repetition by iteration until the solution converges.

The Hypoinverse program calculates the full 4×4 covariance matrix of the solution and derives from it the error ellipsoid containing the horizontal and vertical errors. The error calculation requires an estimate of the variance of the arrival-time data, given as:

$$\sigma^2 = \sigma_r^2 + \gamma\sigma_T^2,$$

where σ_r^2 is the reading-error variance and γ is a weighting factor to include the effect of a poor solution. This second term absorbs misfit due to errors in the velocity model, e.g. the effects of a three-dimensional structure.

4. DATA ACQUISITION AND PROCESSING

4.1 Station logistics and operation

This study is part of the HH2007 project that aims at monitoring acoustic emissions within the Hengill-Hellisheidi geothermal fields. Data was collected in the Hengill-Hellisheidi geothermal area from June 13 to August 13, 2007 using a temporary network covering an area of 220 km^2. The seismograph network comprised of 19 stations (Appendix I) covered in two deployments using 10 Refraction technology (RefTek) 130.01 digital recording instruments and three-channel, 5-second Lennarz seismometers. The recording was continuous with a sample rate of 100 samples/s. Each seismic station consisted of a RefTek seismic data acquisition unit with a flash-card disk, a seismometer, a GPS receiver and was powered by a 12 V battery. The first deployment was in the western part of Hengill while the second deployment was in the eastern part (Figure 7). The acquisition system and batteries were sealed in plastic bags and covered with linoleum to prevent water ingress; all cables were buried as far as possible to prevent the effects of wind noise degrading the signal. Seismometers were placed as close to outcropping rocks as possible in order to avoid noisy conditions and high attenuation associated with tuffs, soils, sediments and other soft surface deposits in order to achieve as high a signal-to-noise ratio as possible. Pits were dug for the seismometers through loose surface cover in areas where outcropping rock was not available in situ. A flat base was then constructed with cement (where needed) for the instrument to be mounted upon. In most cases the instruments were mounted directly on hyaloclastic bedrock. Figure 7 shows the seismic network with recording stations appearing as filled triangles. Information on station names and coordinates can be found in Appendix I.

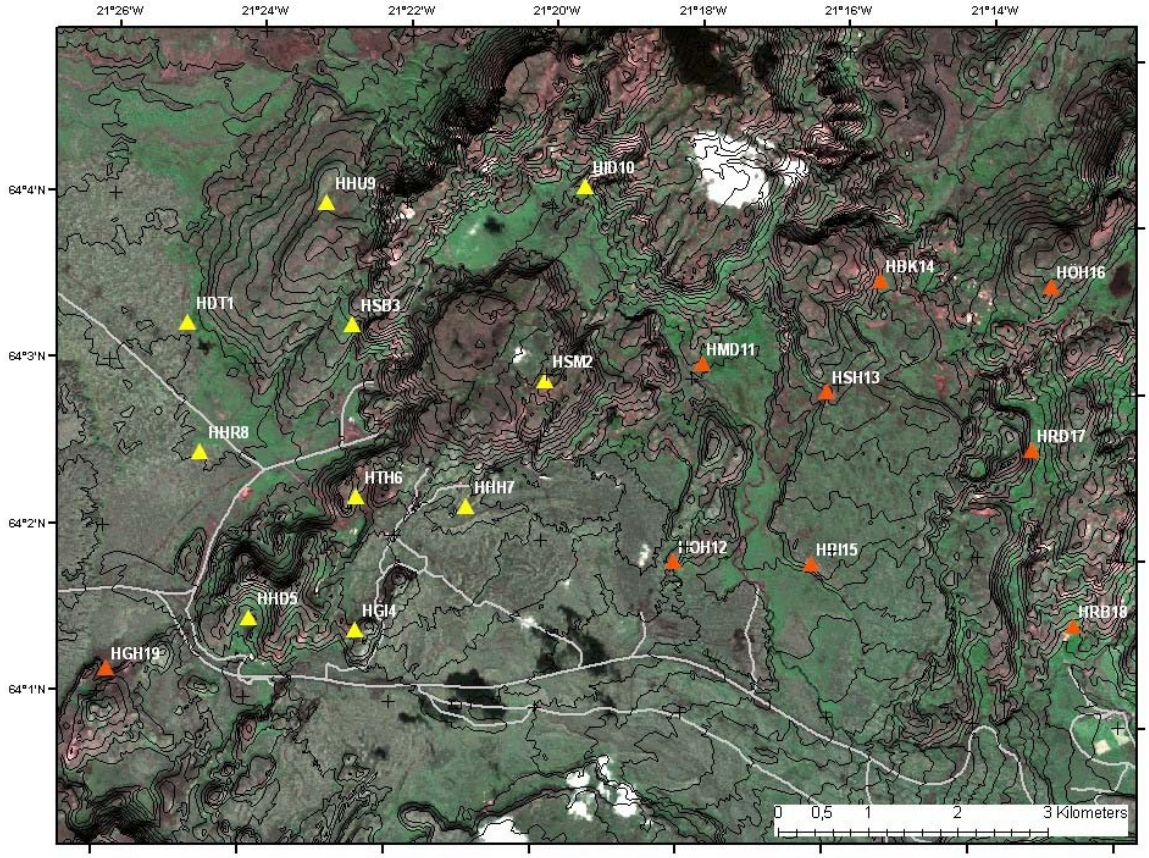

FIGURE 7: The seismic network, light/yellow triangles show the first deployment while dark/orange ones show the second deployment

4.2 Data processing

Data used in this study was recorded by the temporary HH2007 seismic network as well as by the SIL network, which is the permanent regional seismic network in Iceland. Data from the temporary network was downloaded directly from the instrument onto a laptop iMac computer and processed using PASSCAL software. Processing included extracting seismic events from the dataset using a routine extract.csh written by Menke and modified by Brandsdóttir. Data displaying a good signal-to-noise ratio were then analysed using PQL (IRIS, 2007). Picking of the arrival times was done using the PQL program (which has a series of interactive tools such as filtering and spectral frequency display of the waveforms) based on adequate signal-to-noise ratio irrespective of the frequency of the seismic arrival. Accuracy of observed arrival times depends mainly on:

- Accuracy of the station location;
- Sampling interval;
- Accuracy of the time stamp (GPS);
- Phase clarity or impulsiveness.

A total of 60 local events were picked from the dense array yielding 580 P-picks and 530 S-picks. Some high quality data with clear P and S phases were recorded and in such a case picking was easy (Figures 8 and 9). In some cases, it was difficult to distinguish between the P and S phases from the background noise (Figure 10), thus a band pass filter (2 - 8 Hz) was used to filter the noisier events to improve the arrival time estimate (Figure 11).

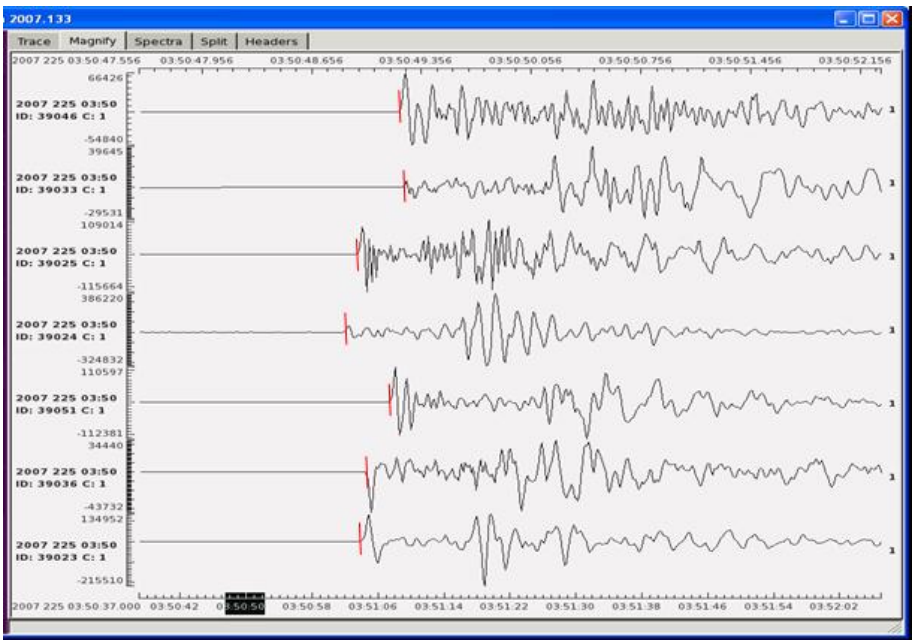

FIGURE 8: Seismograms for an event recorded on August 13, 0350 hrs. showing the vertical component from 7 stations; clear P-wave arrivals can be identified easily and are marked by red/dark solid lines; the black box shows the time span of the seismogram

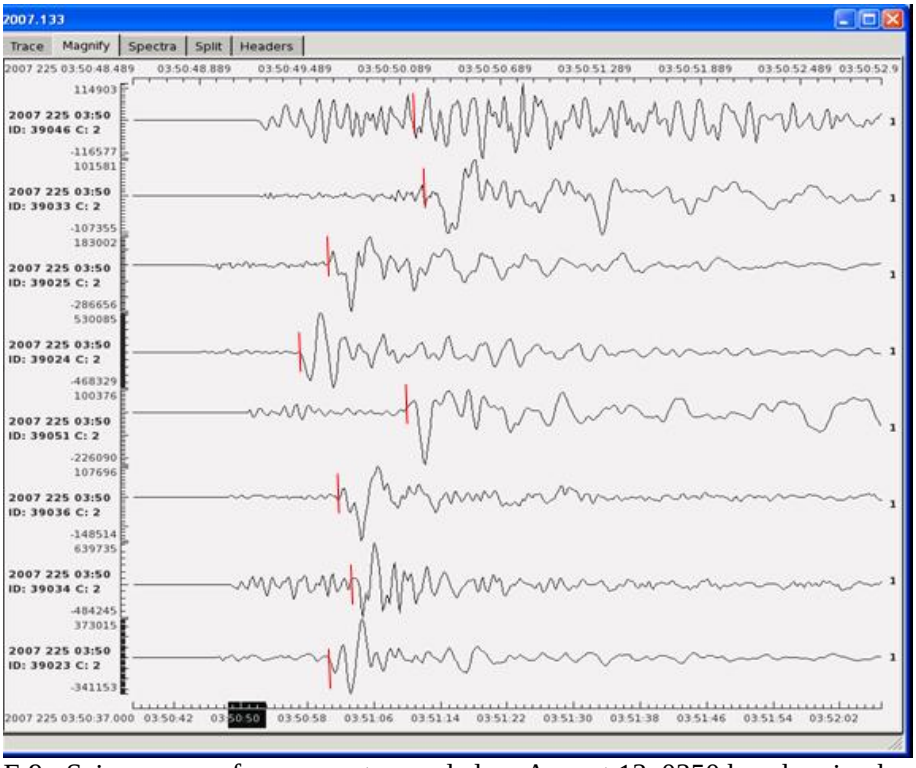

FIGURE 9: Seismograms for an event recorded on August 13, 0350 hrs showing horizontal components from 8 stations; clear S-wave arrivals can be identified easily and are marked by red/dark solid lines. The upper scale is the absolute time

Five different weights (Table 1) were assigned to each arrival (P- and S-wave), based on picking uncertainties. Most of the P-wave arrivals were picked to within 80 ms uncertainty, but most S-wave arrivals had a higher uncertainty of about 120 ms. No S-waves with observation weight 0 and 1 were picked. Additional P and S picks were obtained from the SIL network to aid in accurate location of events.

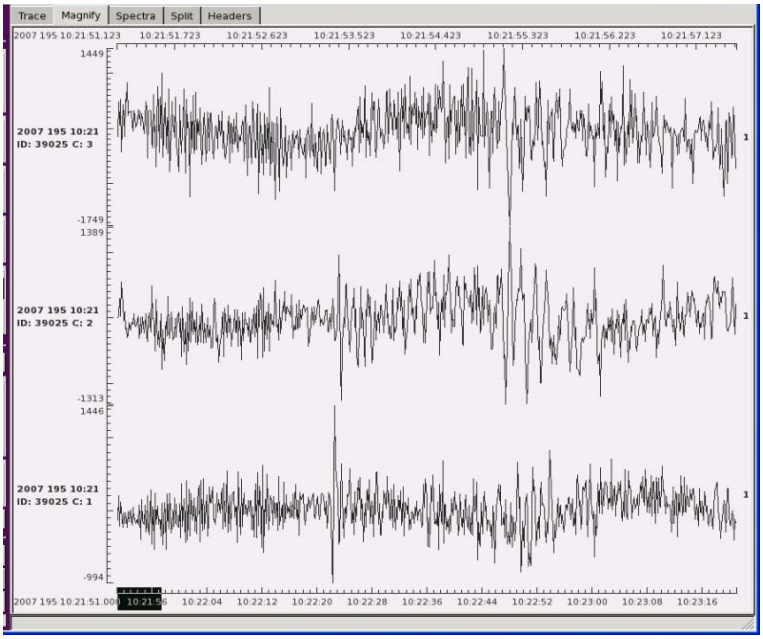

FIGURE 10: Seismograms showing high frequency noise that masks the P and S arrival times (before filtering); the upper scale is the absolute time

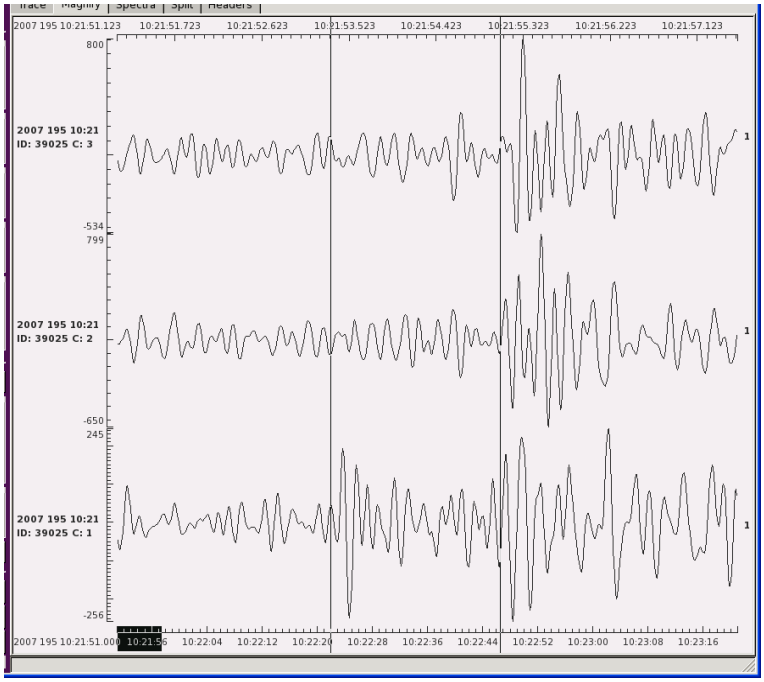

FIGURE 11: Seismograms showing clear P- and S-phases after band pass (2-8 Hz) filtering of the signals shown on Figure 10; the two vertical lines delineate the P and S phases, respectively

TABLE 1: Weights assigned to travel time picks (P- and S-wave arrival times); these weights are used by the location program to reflect the arrival quality

Weight	Number of P-picks	P-pick clarity	Number of S-picks	S-pick clarity
0 = Full weight	490	Very clear	-	-
1 = Weight	50	Clear	-	-
2 = Half weight	25	Almost clear	400	Clear
3 = Quarter weight	10	Unclear	95	Unclear
4 = No weight	5	Poor	35	Poor

Hypoinverse assumes that the recording stations are situated on a horizontal surface (above a plane-layered velocity model) and station elevations are not used. In the crustal model, velocity can vary only with depth. A simple velocity model was used with linear velocity gradients within layers and no velocity discontinuities (Figure 12). With linear gradients, the discontinuities in travel-time derivatives caused by a discontinuous velocity profile are smoothed out. This is the model normally used for locating earthquakes with the Icelandic SIL system. The elevation range for the 19 observation sites is about ±200 m corresponding to a travel time of about ±100 ms, which is comparable to the picking uncertainty.

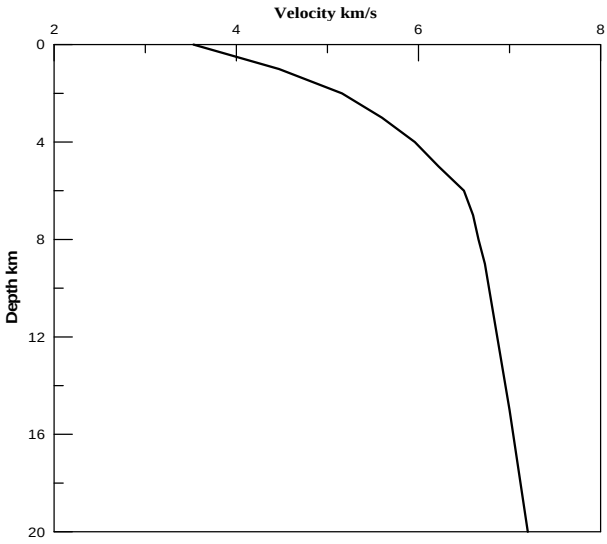

FIGURE 12: Linear-gradient crustal velocity model used to derive the locations

4.3 Seismicity in the period of June 13 – August 13, 2007

More than 60 events were recorded during our two month field campaign. A total of 60 events were located using data from the two station deployments (Appendix II). The first array was deployed June 13-21 and the second array July 26-28. Earthquakes through August 13th were located. Fewer events were located during the second deployment. In order to obtain a reliable comparison with the earthquake locations from the automated SIL network, the SIL velocity model was used. By comparison of our locations with the SIL network locations, precision of location improved by a factor of about 2. Both the epicentre and hypocentre locations were better constrained in our case than in the SIL locations. Table 2 shows few examples of the variation in depth of our locations and the SIL locations. SIL´s vertical errors are considerably higher. The shallowest earthquake located by the network was 0.8 km while the shallowest SIL hypocenter was at 3.1 km.

TABLE 2: Depth comparison of locations made using the same model by different networks

Event time	Our locations		SIL locations	
	Depth (km)	Vertical error (km)	Depth (km)	Vertical error (km)
20070616 0138	6.6	0.4	5.9	0.4
20070619 0411	5.4	0.3	5.2	0.6
20070707 0212	4.8	0.3	6.6	1.0
20070714 1021	6.0	0.5	6.2	0.8
20070721 0539	6.1	0.5	5.3	1.7
20070725 1254	0.8	0.3	3.1	0.8
20070728 0123	8.5	0.5	8.0	0.5
20070731 0727	5.1	0.2	2.0	1.2
20070809 1316	6.7	0.4	7.0	0.4
20070811 1339	4.4	0.1	5.6	0.7
20070813 0350	4.5	0.2	5.6	0.7

The HYPOINVERSE locations had an average horizontal error of 0.27 km and a vertical error of 0.6 km as opposed to the SIL locations which had horizontal error of 1 km and vertical error of 2 km. The root mean square (RMS) varied from 0.00 to 0.07 except in 4 events that had RMS of 0.11. The earthquake location quality was classified (by the location program) with letters a, b, c, and d

representing excellent, good, fair and poor locations, respectively. Most of the events located (80%) had excellent or good locations while the rest (20%) had fair or poor locations. It is evident that our locations were better constrained than the SIL locations owing to the fact that a dense array was used. Magnitudes were not determined for the events located but by correlating them with the SIL earthquakes, the majority of the earthquakes had magnitudes in the range of 0.1–2 Mo though some few events (5) had magnitudes 2 and above.

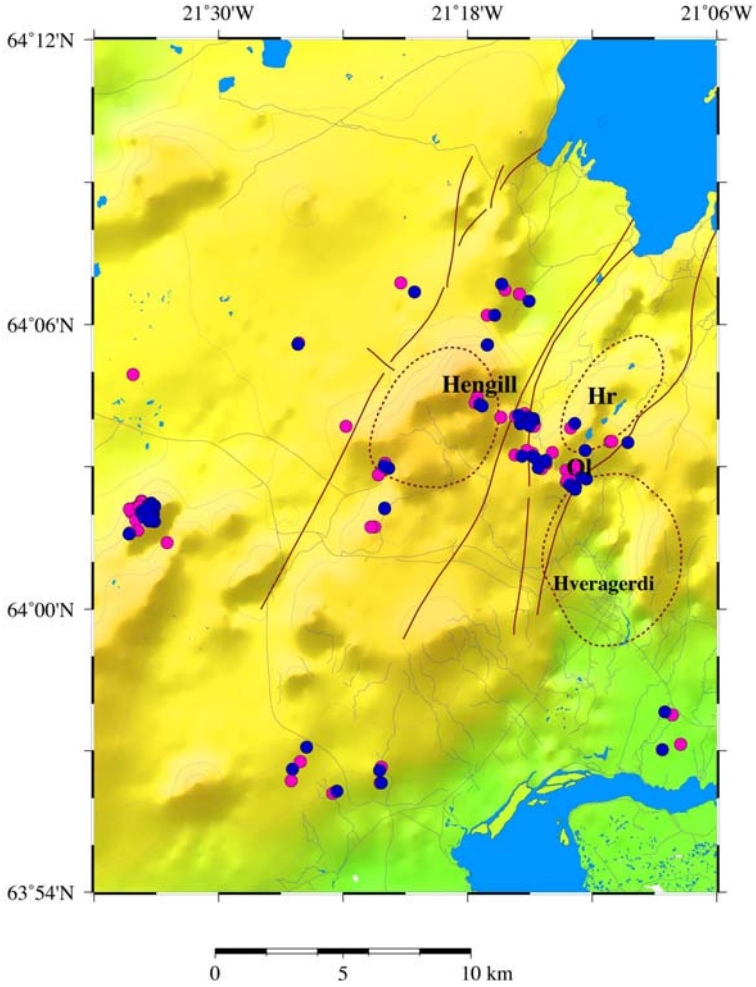

FIGURE 13: Locations of 60 earthquakes in Hengill-Hellisheidi area in relation to the volcanic systems. Red (dark) circles show epicentre locations based on the local temporary network and the SIL network, while blue (lighter) ones show locations from the regional SIL network. Red (dark) solid lines show the volcanic system and dotted red (dark) lines show central volcanoes

Seismicity in the Hengill area during the period of June 13 to August 13 was rather low (Figure 13) as compared to previous records in the same time frame. On average, there were 2 events per day. Most of the events within our study area followed an almost linear NW-SE trend across Ölkelduháls (Figure 13) or fell within the NE-SW trending Hengill fissure swarm. In both cases, they seemed to closely correlate with surface geothermal activity. A cluster southwest of Hengill belonged to a swarm by Mt. Vífilfell in June.

Although most earthquakes occurred predominantly along a NW-SE trend, some events also occurred along the NE-SW trending fissure swarm.

There is a strong correlation between the earthquake locations, geothermal manifestations and the tectonic features (Figures 14 and 15). Hypocenters east of 21.3°W cluster at 4-6 km depth along a NW-SE seismic belt whereas hypocenters parallel to the NE-SW fissure swarm have a higher depth range, 0-9 km (Figures 16 and 17). The same epicentral distribution was obtained using old crustal models derived for the Reykjanes Peninsula and Krafla region although the earthquake hypocenters varied by up to 0.5 km. Another short earthquake survey in August-September 1999 revealed a similar epicentral and depth distribution of microearthquakes within the study area with most of the hypocenters clustering at 3.5-5.3 km depth within the Hrómundartindur system and Ölkelduháls, but 4-8 km depth south of Hengill (Allen, 2001). A master event relocation of 10 events indicated that the Hrómundartindur events occurred at 5.5 km depth along a N-S striking lineament. A focal mechanism of the master event indicated right-lateral strike-slip movement with a normal component along a N30°E striking fault (Allen, 2001).

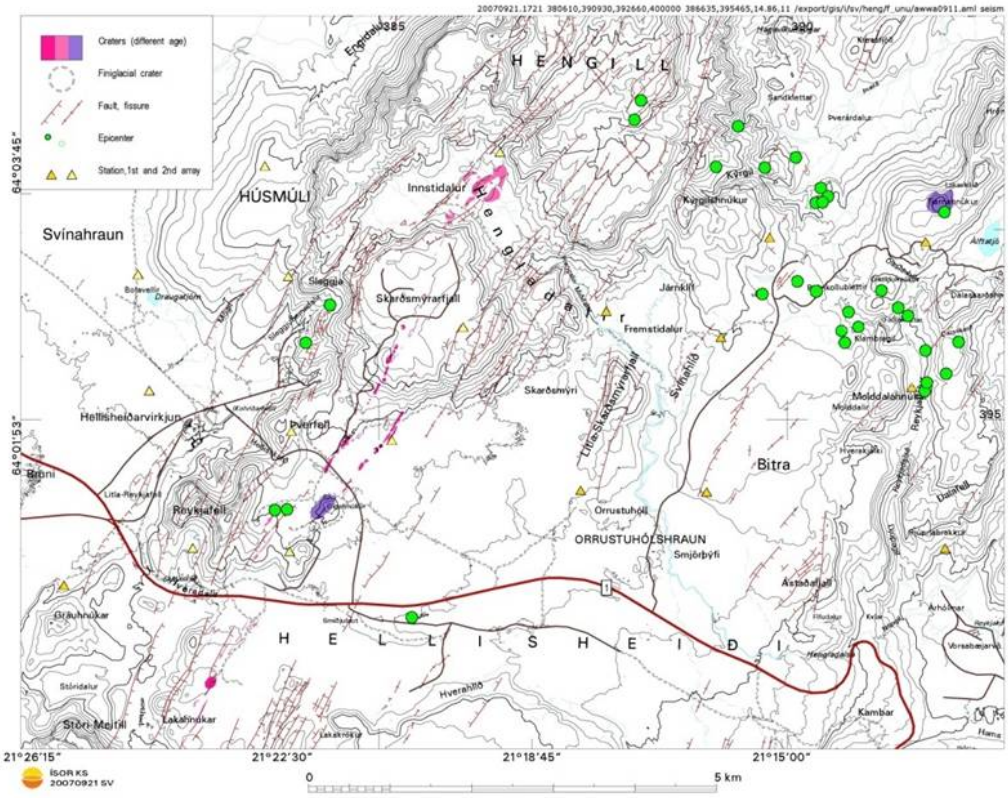

FIGURE 14: Epicentre locations of 31 earthquakes and structures in the study area; green (gray) circles show epicentres and yellow (light) triangles show the stations

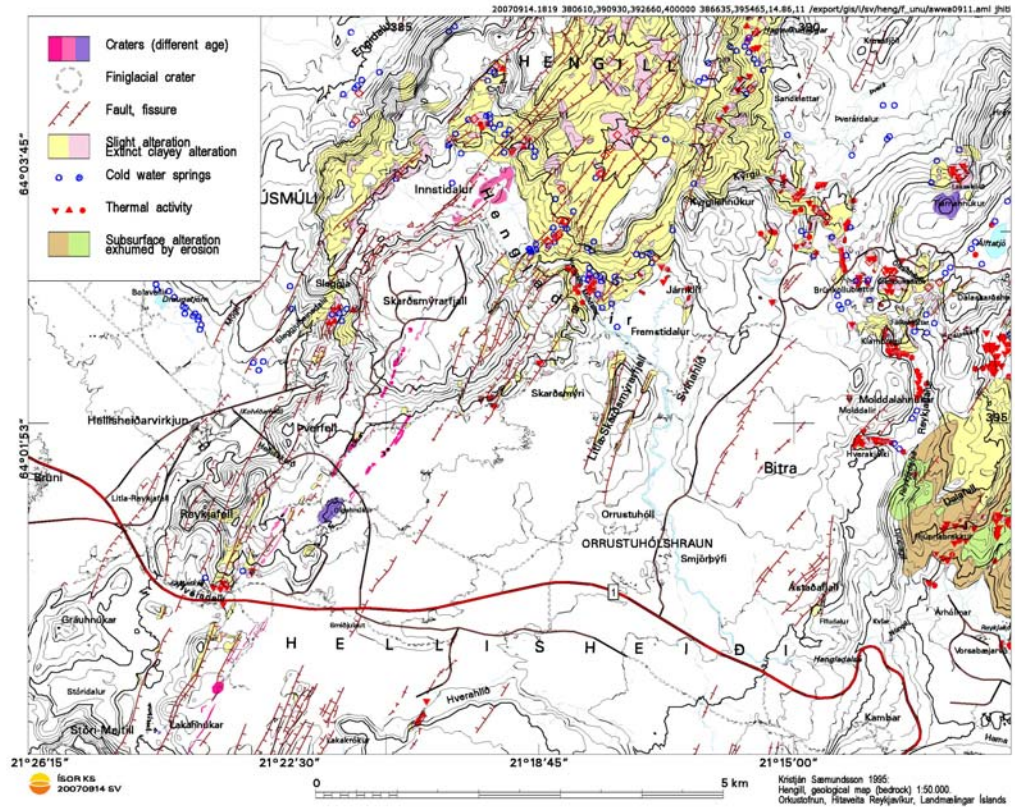

FIGURE 15: Geothermal activity, alteration and major tectonic features of the study area (Saemundsson, K., 1995b)

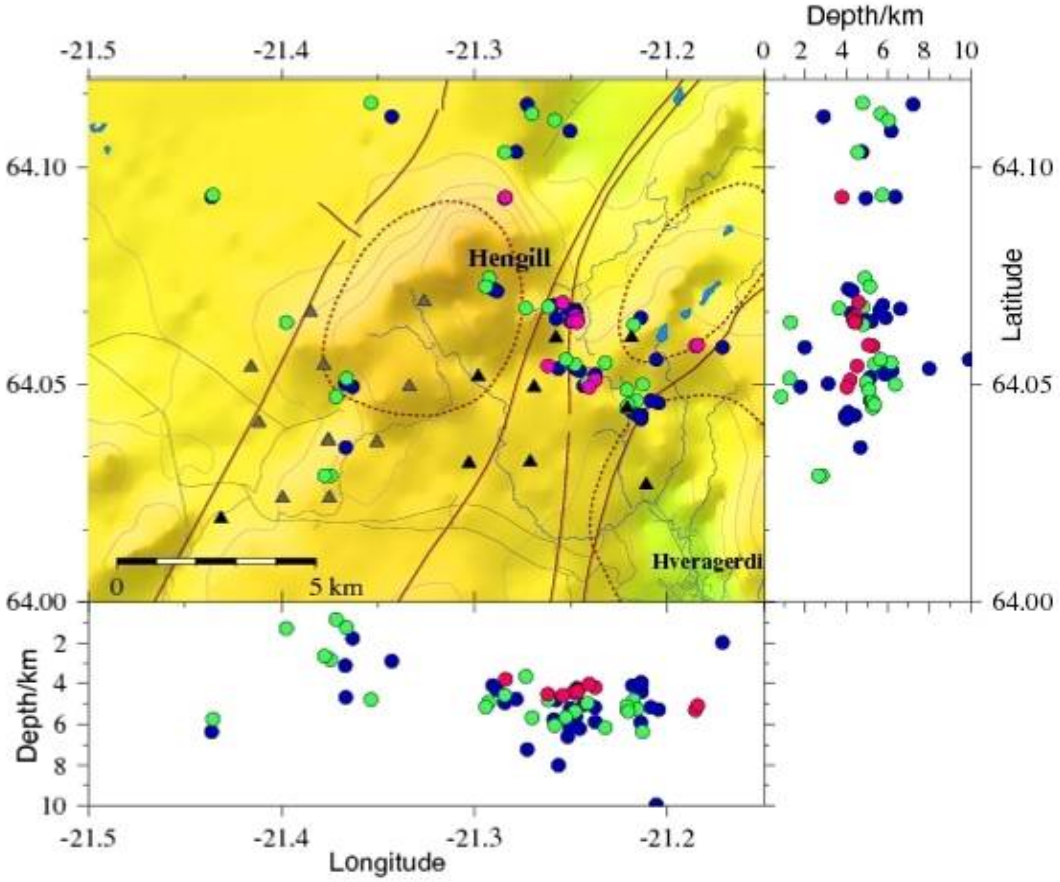

FIGURE 16: Epicentre locations of 31 events in the area; red (dark) and green (gray) coloured circles represent our locations while blue (light gray) ones represent SIL's. Grey and black triangles represent our stations (first and second deployment, respectively). Right and bottom show variation in depths with latitude and longitude, respectively. The red (dark) solid lines show the volcanic systems while the dotted ones show the central volcanoes

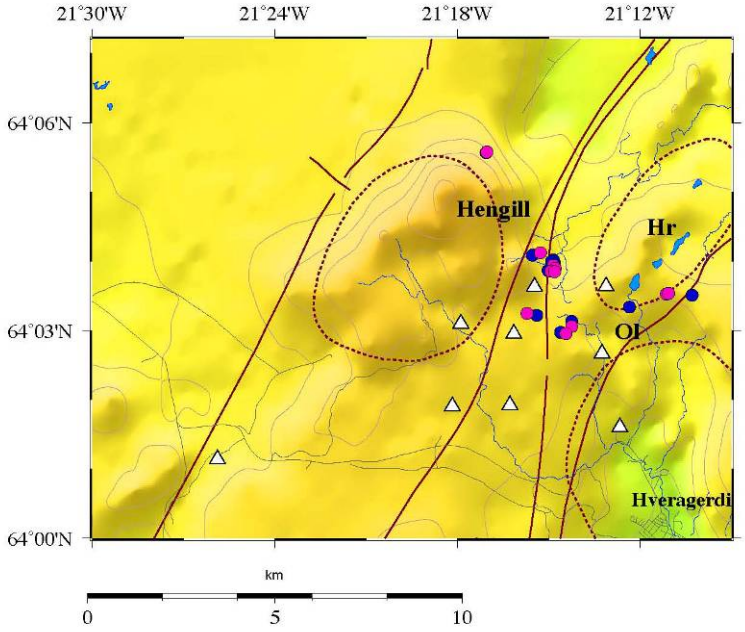

FIGURE 17: Epicentre locations of 10 events in the area located by the 2nd array. Red (dark) coloured circles represent our locations while blue (lighter) ones represent SIL's locations; white triangles represent the stations

Tectonic and topographic evidence of an active fault zone following a NW-SE trend from Grensdalur across Ölkelduháls to Hengill may be indicative of tensile shearing and high permeability with relatively high seismicity and geothermal activity. Without focal solutions, it is not possible to determine the nature of this earthquake activity and it can only be speculated that tectonic activity coupled with fluid movements might be causing the seismicity. However, increased geothermal activity following the seismic activity within the Hengill region during 1994-1998 and the SISZ earthquakes in June, 2000 lends further evidence to the link between seismicity and increased permeability (Björnsson et al., 2001; Jónsson et al., 2003).

Fewer events were recorded during the second deployment. The second array was deployed 26th July thus there was no time to analyse much of the data as the study period was short. Ten earthquakes were located on the second array and all the earthquakes (Figure 17) followed the same trend (NW-SE). It is clear that there is some mechanism controlling these earthquakes, possibly fluid flow and tectonics. It is during this time that the deepest located earthquake was recorded, at a depth of 8.85 km on 28th July. The majority of the hypocenters during the second deployment were in the depth range of 4-5 km.

A peculiar swarm occurred on July 24, 2007, consisting of numerous microearthquakes increasing gradually in size between 2100 and 2210 hrs. and reaching a Mo magnitude of 1.6 according to the SIL network (Figure 18). The swarm originated at Ölkelduháls. Similar swarms have been observed in geothermal fields and have been explained as resulting from cooling contraction due to circulating groundwater in hot rock at depth (Sigmundsson et al., 1997). Stefánsson et al. (2006) proposed that frequent but minor seismic swarms within the SISZ could be related to upwelling fluids.

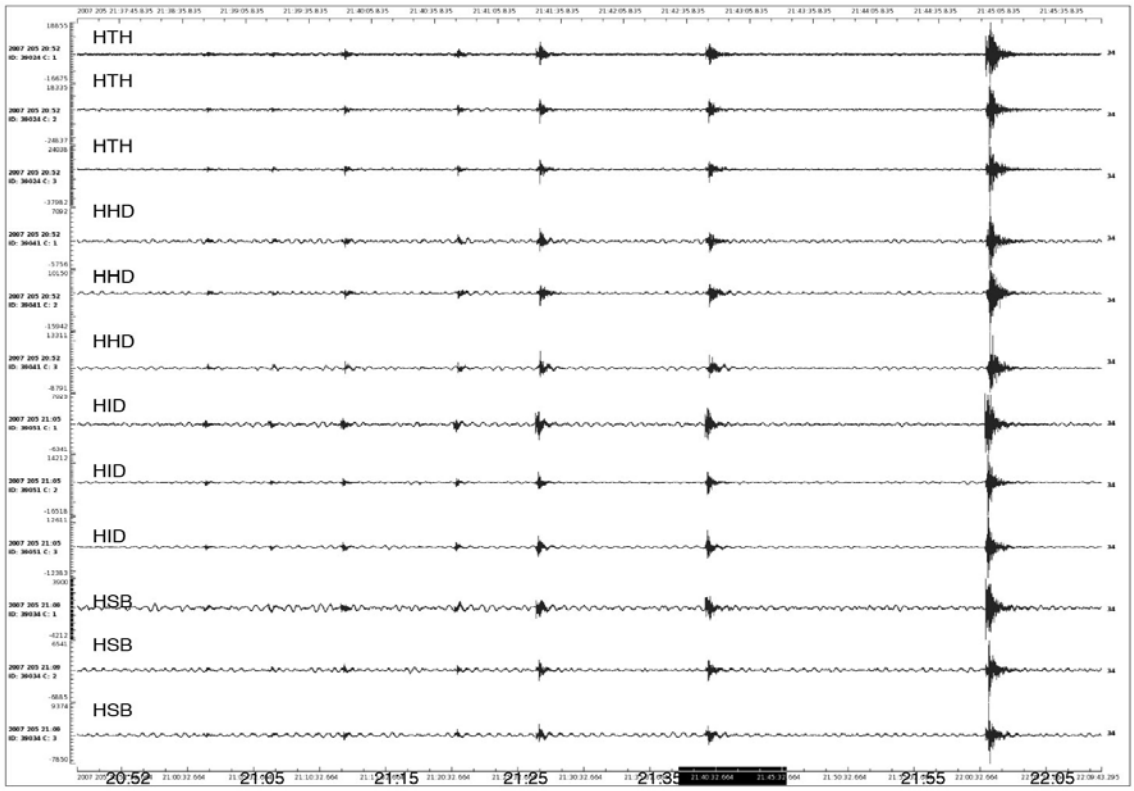

FIGURE 18: Plot of the earthquake swarm that occurred on July 23 at 2100-2210 hrs. at Ölkelduháls area; the station code is indicated on the left and time is written in bold at the bottom

4.4 Seismic noise

With increased emphasis on geothermal development, new exploration methods are needed in order to improve the general understanding of geothermal reservoirs, characterize their extent and assess the potential for sustainable utilization. Monitoring of acoustic emissions within geothermal areas may provide a new tool for evaluating the spatial extent of geothermal fields and modelling rock-fluid interactions. Three-dimensional seismic data have been used to assess the spatial and temporal distribution of noise within several high-temperature geothermal fields in Iceland. Seismic noise in the 4-6 Hz range within the Svartsengi field can be attributed to steam hydraulics and pressure oscillations within geothermal reservoirs (Brandsdóttir et al., 1994). Seismic noise surveys compliment electrical resistivity soundings and TEM-surveys by providing information pertinent to the current geothermal activity and the extent of steam fields within the uppermost crust of the geothermal reservoir. Information related to acoustic emissions can, thus, help define targets for future wells.

A preliminary survey of spectral peaks at a few of the HH2007 stations showed 8-30 Hz peaks to have the most energy close to blowing boreholes, such as HBK (Brúnkollublettir), where they are more than 30 times higher in amplitude than elsewhere. The frequency of this noise falls in the same range as observed within Svartsengi and was attributed to boreholes there (Brandsdóttir et al., 1994). The source of peculiar spectral peaks at 8-10 Hz and close to 15 Hz at station HGH (Gráuhnjúkar) remains unresolved (Figure 19), they may, however, be associated with wastewater injection close to the HGH site.

The preliminary study of the temporal noise distribution within the Hellisheidi geothermal fields revealed 4-6 Hz spectral peaks at stations located in the vicinity of surface geothermal activity (Figure 20). Noise spectra in the frequency range 2-7 Hz bring out the noise levels thought to be associated with geothermal activity. Surface geothermal activity is evident in the vicinity of stations HSH, HRB, HOL and HBK. All these stations exhibit spectral peaks in the 4-6 Hz range. In addition, a peculiar peak at 2.5 Hz is observed at HRB (Rjúpnabrekkur) station, located within a geothermal field and at 3.5 Hz at HOL (Ölkelduháls) and HSH (Svínahlíd).

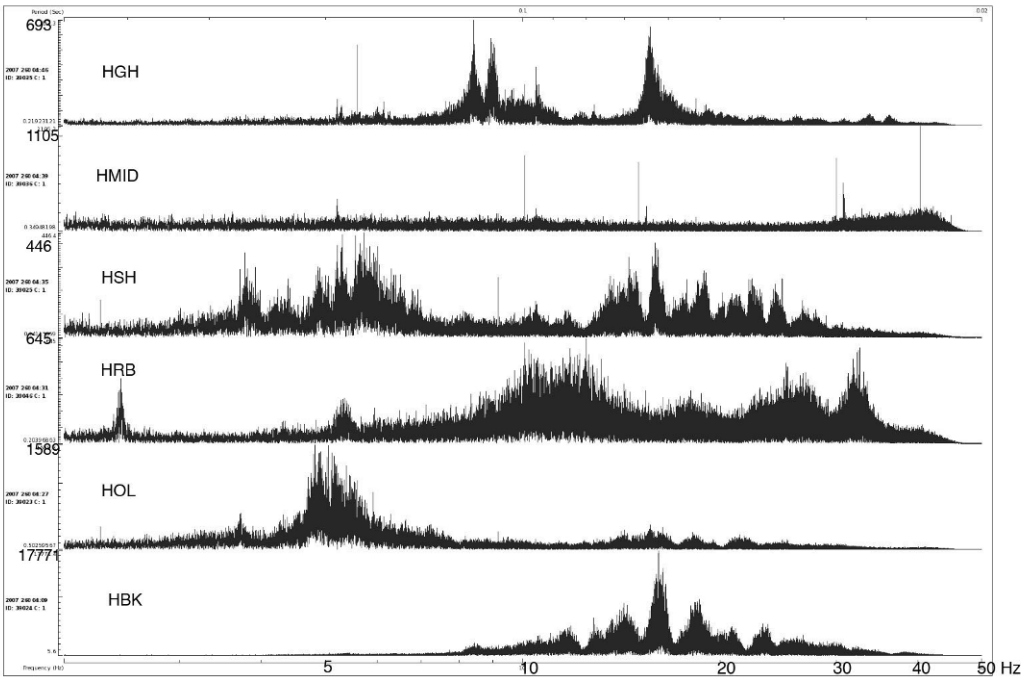

FIGURE 19: Spectral plots of 6 stations on a calm morning (Sept 10); it is a 20 minute average plot between 2 and 50 HZ; note the variations in noise levels, shown in counts on the Y axis

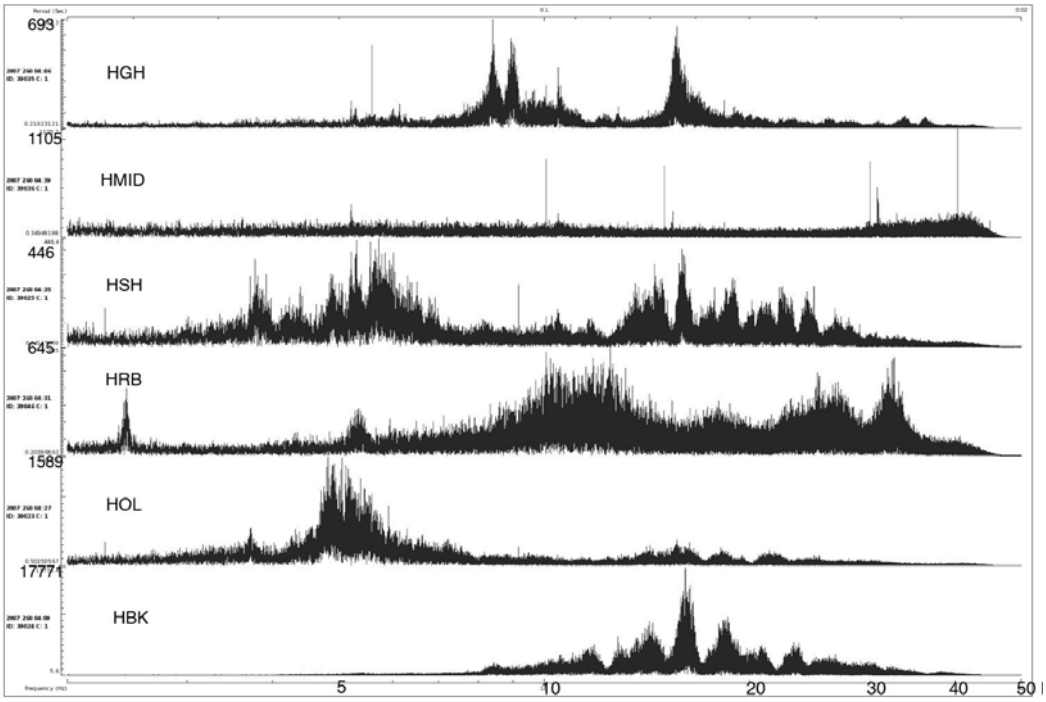

FIGURE 20: Spectral plots of 6 stations on a calm (no wind) morning (Sept 10); it is a 5 minute average plot filtered between 2 and 7 HZ to eliminate borehole noise at HBK and water fall noise at HRB

Some of the noise observed can be correlated with weather (wind) and with open (blowing) holes. The sharp spikes observed are more likely to be of artificial origin than of natural causes. The spikes could also be caused by rain on the sensor from drops of condensed vapour forming within the bucket protecting the sensor. Broader spectral peaks are more likely related to a natural process or source, which have not yet been established. More detailed surveying is needed in the vicinity of each geothermal location in order to determine the source of these signals.

4. DISCUSSION AND CONCLUSIONS

The extensive high-temperature geothermal area studied encompasses the Hengill, Hrómundartindur and Grensdalur central volcanoes. The whole area displays a continuous background of small magnitude earthquake activity that correlates spatially with surface heat loss (Foulger, 1988a and b). Of the geothermal reservoirs in the Hengill area, the one below Ölkelduháls has been shown by geochemical studies to have maxima of 300-310°C (Torfason et al., 1983). Ölkelduháls is an area with intense surface geothermal activity. Although seismic activity varies with time, the seismicity map presented in this paper is in some ways similar to most maps produced by different scientists who have worked in the area. Ward and Björnsson (1971), Foulger and Einarsson (1980), and Rögnvaldsson et al. (1998) presented seismic maps dominated by a cluster about 6-10 km southeast of Hengill. Ward and Foulger concluded that the seismicity was due to contraction cracking associated with cooling and circulating groundwater while Rögnvaldsson et al. concluded that ductile motion at depth might be the source of the earthquakes coupled with tectonic movements. However, Rögnvaldsson et al. (1998) gave an alternative hypothesis that the earthquakes were caused by dilation in the presence of high fluid pressure.

It is premature to decide conclusively the cause of microearthquakes in the study region, based on the relatively small number of events that occurred during the study period. Most earthquakes occurred near Ölkelduháls, which is a highly active high-temperature geothermal field. Thus, fluids play a

probable role in the mechanism. Deeper earthquakes, in a range 4-6 km, occurred at Ölkelduháls while shallower earthquakes occurred elsewhere in the Hengill fissure swarm. This suggests that both hydraulic fracturing and tectonic activity controlled the occurrence of the earthquakes. The fact that no earthquakes occurred deeper than 7.5 km has been taken as an indicator of the brittle-ductile boundary (Stefánsson et al., 1993).

No focal mechanisms were determined for the earthquakes. Thus, the type of faulting in the area could not be concluded. During the period between 1993 and 1996, the dominant type of faulting in the area, determined from fault plane solutions of more than 10,000 microearthquakes, was strike-slip (Rögnvaldsson et al., 1998). Rögnvaldsson et al. (1999) reported that at Ölkelduháls (from January 1 to May 20, 1998), fault plane solutions showed a combination of right-lateral strike-slip and normal faulting. Miller et al. (1998) reported that about 75% of the earthquakes in the Hengill-Grensdalur area have non double-couple radiation patterns and are interpreted as being due to tensile crack formation within the heat source of the geothermal fields. Tryggvason et al. (2002) observed that at a depth of 4-10 km below the Hengill area, the velocity of P- and S-waves is reduced, more for P-waves than S-waves (low Vp/Vs). This is interpreted as a heavily fractured volcanic fissure system and the low velocities are caused by supercritical fluids, some of magmatic origin. All the above arguments show that there is a conflict as to the cause of the earthquakes in the Hengill area.

In conclusion, it is observed that most of the earthquakes during the study period are strongly correlated with geothermal activity. More analysis of the data is called for in order to confidently interpret them. Fault plane solutions should be determined for the earthquakes so as to confidently determine the source of the earthquakes. Analysis of geothermal noise should be emphasized to discover sources of the spectral peaks at 2.5-6 Hz. This might indicate fluid flow. Shear-wave attenuation should also be analysed.

ACKNOWLEDGEMENTS

I thank the almighty father for granting me good health and the grace to start and finish this course. My sincere thanks go to UNU-GTP and Government of Iceland for granting me the opportunity to take part in this important course and for financing it. Special thanks go to the staff of UNU Geothermal Training Programme, Dr. Ingvar B. Fridleifsson, Mr. Lúdvík S. Georgsson, Ms. Thórhildur Ísberg and Ms. Dorthe H. Holm, for their organisation and endless efforts to assist me in every way during the entire period. I am grateful to the entire ÍSOR and Orkustofnun (National Energy Authority of Iceland) staff for sharing their knowledge and experience. The University of Nairobi is acknowledged for granting me permission to take part in this course and Kenya Electricity Generating company (KenGen) for nominating me for the course.

My heartfelt gratitude goes to my supervisors, Mrs. Bryndís Brandsdóttir of the Institute of Earth Sciences, University of Iceland, and Mr. Kristján Agústsson of ÍSOR for all the seismological knowledge and experience they shared with me. Really, I am much honoured to have been your student and to learn more in the field of applied seismology. It was interesting and fun being supervised by you. The assistance of Dr. Ólafur Gudmundsson of the Institute of Earth Sciences, University of Iceland is also greatly acknowledged. The GMT public domain software and Arc GIS were used to generate maps with the help of Bryndís Brandsdóttir, Ingibjörg Jónsdóttir (Askja) and Skúli Víkingsson (ÍSOR).

My deepest gratitude goes to my family and friends for their unconditional support and best wishes during my stay in Iceland. Thanks to the 2007 UNU Fellows for all the ideas we shared and exchanged during the entire period and for making my entire stay in Iceland fun. It was a pleasure meeting and interacting with all of you.

REFERENCES

Ágústsson, K., and Halldórsson, P., 2005: *Seismic hazard in the Hengill area based on the SIL earthquake catalogue - First results*. Vedurstofa Íslands, report 05015, 42 pp.

Allen, C., 2001: *The seismicity of the Hengill triple junction, Iceland*. St. Catharine´s College, Cambridge, unpubl. report 62 pp.

Árnason, K., 1993: Relation between resistivity and geothermal activity in basaltic rocks. English translation of a chapter in: *Geothermal activity at the Ölkelduháls field, resistivity soundings in 1991 and 1992*. Orkustofnun, Reykjavík, report OS-93037/JHD-10 (in Icelandic), 82 pp.

Árnason, B., Theodórsson, P., Björnsson, S., and Saemundsson, K., 1967: Hengill, a high-temperature thermal area in Iceland. *Bull. Volcanologique, XXXIII-1*, 245-260.

Bjarnason, I.Th., Menke, W., Flóvenz, Ó.G., and Caress, D., 1993: Tomographic image of the Mid-Atlantic plate boundary in southwestern Iceland. *J. Geophys. Res., 98*, 6607–6622.

Björnsson, A., Hersir, G.P., and Björnsson, G., 1986: The Hengill high temperature area, SW-Iceland: Regional geophysical survey. *Geoth. Res. Council, Transactions, 10*, 205-210.

Björnsson, G., Saemundsson, K., Flóvenz, Ó.G., and Einarsson, E.M., 2001: Pre- and post-hydrological pressure signals associated with two large earthquakes in S-Iceland in June 2000 (in Icelandic). *Geological Society of Iceland, Spring Conference 2001, Abstracts*, 1 pp.

Bödvarsson, G.S., Björnsson, S., Gunnarsson, Á., Gunnlaugsson, E., Sigurdsson, Ó., Stefánsson V., and Steingrímsson, B., 1990: The Nesjavellir geothermal field, Iceland. Part 1. Field characteristics and development of a three-dimensional numerical model. *J. Geotherm. Sci. and Tech., 2-3*, 189-228.

Bolt, B.A., 2004: *Earthquakes* (5th edition). W.H. Freeman and Co, NY, 378 pp.

Brandsdóttir, B., Einarsson, P., Árnason,. K., and Kristmannsdóttir, H., 1994: *Refraction measurements and seismic monitoring during an injection experiment at the Svartsengi geothermal field in 1993.* Orkustofnun, Reykjavík, report OS-94016/JHD-05 & RH-03-94 (in Icelandic with an English summary), 28 pp.

Clifton, A. and Einarsson, P., 2005: Styles of surface rupture accompanying the June 17 and 21, 2000 earthquakes in the South Iceland seismic zone. *Tectonophysics, 396*, 141-159.

Clifton, E.A., Sigmundsson, F., Feigl, K.L., Gudmundsson, G., and Árnadóttir, T., 2002: Surface effects of faulting and deformation resulting from magma accumulation at the Hengill triple junction, SW Iceland, 1994 – 1998. *J. Volc. and Geothermal Res., 115*, 233-255.

DeMetz, C., Gordon, R.G., Argus, D.F., and Stein, S., 1994: Effect of recent revision to the geomagnetic reversal time scale on estimates of current plate motions. *Geophysical Research Letters, 21*, 2191-2194.

Einarsson, P., 1991. Earthquakes and present-day tectonism in Iceland. In: Björnsson, S., Gregersen, S., Husebye, E.S., Korhonen, H., and Lund, C.E. (editors), Imaging and understanding the lithosphere of Scandinavia and Iceland. *Tectonophysics*, 189, 261-279.

Einarsson, P., and Brandsdóttir, B., 2000: Earthquakes in the Mýrdalsjökull area, Iceland, 1978-1985: Seasonal correlation and relation to volcanoes. *Jökull, 49*, 59-74.

Einarsson P. and Saemundsson, K., 1987: Earthquake epicentres 1982–1985 and volcanic systems in Iceland. A map in: Sigfússon Th. (ed.), *As a matter of fact*. Festschrift for Thorbjörn Sigurgeirsson (in Icelandic), Menningarsjódur, Reykjavík.

Feigl, K., Gasperi, J., Sigmundsson, F., and Rigo, A., 2000: Crustal deformation near Hengill volcano, Iceland 1993-1998: Coupling between volcanism and faulting inferred from elastic modelling of satellite radar interferograms. *J. Geophys. Res., 105,* 25,655-25,670.

Foulger, G., and Einarsson, P., 1980: Recent earthquakes in the Hengill-Hellisheidi area in SW-Iceland. *J. Geophys., 47*, 171-175.

Foulger, G.R., 1988a: Hengill triple junction, SW-Iceland, 1. Tectonic structure and the spatial and temporal distribution of local earthquakes. *J. Geophys. Res., 93-B11,* 13,493-13,506.

Foulger, G.R., 1988b: Hengill triple junction, SW-Iceland, 2. Anomalous earthquake focal mechanisms and implications for process within the geothermal reservoir and at accretionary plate boundaries. *J. Geophys. Res., 93-B11,* 13,507-13,523.

Foulger, G.R., and Toomey, D.R., 1989: Structure and evolution of the Hengill-Grensdalur volcanic complex, Iceland: Geology, geophysics and seismic tomography. *J. Geophys. Res., 94-B12,* 17,511-17,522.

Fridleifsson I.B., and Freeston, D.H., 1994: Geothermal energy research and development. *Geothermics, 23-2*, 175-214.

Fridleifsson, G.Ó., Ármannsson, H., Árnason, K., Bjarnason, I.Th., and Gíslason, G., 2003: Part I: Geosciences and site selection. In: Fridleifsson, G.Ó. (ed.), *Iceland Deep Drilling Project, feasibility report.* Orkustofnun, Reykjavík, report OS-2003-007, 104 pp.

Friese, N., Krumbholz, M., Burchardt, S., and Gudmundsson, A., 2005: Tectonics of the Hengill volcano, Southwest Iceland. *American Geophysical Union, Fall Meeting 2005, abstracts.*

Geothermal Education Office, 2007: Geothermal Education Office, Internet website: *www.geothermal.marin.org*

Hackman, M.C., King, G.C.P., and Bilham, R., 1990: The mechanics of the South Iceland seismic zone. *J. Geophys. Res., 95*, 17,339-17,351.

Hersir, G.P., and Björnsson, A., 1991: *Geophysical exploration for geothermal resources, principles and application.* UNU-GTP, Iceland, report 15, 94 pp.

IRIS, 2007: *Passcal program*. Incorporated Research Institution for Seismology. Internet website: *www.passcal.nmt.edu.*

Jakobsdóttir, S.J., Gudmundsson, G.B., and Stefánsson, R., 2002: Seismicity in Iceland 1991-2000 monitored by the SIL seismic system. *Jökull, 51*, 87-94.

Jónsson, S., Segall, P., Pedersen, R., and Björnsson, G., 2003: Post-earthquake ground movements correlated to pore-pressure transients. *Nature, 424*, 179-183.

Klein, F.W., 2000: *User´s guide to HYPOINVERSE-2000, a Fortran program to solve for earthquake locations and magnitudes*. U.S. Geological Survey, open file report 02-171, 123 pp.

Lay, T., and Wallace, C.T., 1995: *Modern global seismology*. Academic Press, NY, 521 pp.

Lee, W.H.K., and Stewart, S.W., 1981: *Principles and applications of microearthquake networks*. Academic Press, NY, 293 pp.

Menke, W., 1984: *Geophysical data analysis: Discrete inverse theory*. Academic Press, Inc., NY, 235 pp.

Miller, A.D., Julian, B.R., and Foulger, G.R., 1998: Three-dimensional seismic structure and moment tensor of non-double-couple earthquakes at the Hengill-Grensdalur volcanic complex, Iceland. *Geophys J. Int., 133,* 309-325.

Press, F., and Siever, R., 1974: *Earth.* Freeman and Co., SF, 945 pp.

Reykjavík Energy, 2007: *Nesjavellir power plant.* Reykjavík Energy, brochure.

Rögnvaldsson, S.Th., Gudmundsson, G.B., Ágústsson, K., Jakobsdóttir, S.S., Slunga, R., and Stefánsson, R., 1998: *Overview of the 1993-1996 seismicity near Hengill*. Vedurstofa Íslands, report VÍ-R98006-JA05, Reykjavík, 16 pp.

Rögnvaldsson, S.Th., Vogfjörd, K.S., and Slunga, R., 1999: *Mapping of faults in the Hengill area with microearthquakes* (in Icelandic). Vedurstofa Íslands, report VÍ-R99002-JA01, Reykjavík, 18 pp.

Saemundsson, K., 1978: Fissure swarms and central volcanoes of the neovolcanic zones of Iceland. *Geol. J., Sp. issue, 10,* 415-432.

Saemundsson, K., 1979: Outline of the geology of Iceland. *Jökull, 29,* 7-28.

Saemundsson, K., 1995a: *Geological map of the Hengill area 1:50,000*. Orkustofnun, Reykjavík.

Saemundsson, K., 1995b: *Geothermal and hydrothermal map of the Hengill area, 1:25,000.* Orkustofnun, Reykjavík.

Saemundsson, K., and Fridleifsson I.B., 1980: Application of geology in geothermal research inIceland (in Icelandic with English summary). *Náttúrufraedingurinn, 50-3/4,* 157-188.

Sigmundsson, F., Einarsson, P., Rögnvaldsson, S.T., Foulger G.R., Hodgkinsson, K.M., and Thorbergsson, G., 1997: The 1994-1995 seismicity and deformation at the Hengill triple junction, Iceland: triggering of earthquakes by minor magma injection in a zone of horizontal shear stress. *J. Geophys. Res., 102-B7,* 15151-15161.

Stefánsson, R., Bödvarsson, R., Slunga, R., Einarsson, P., Jakobsdóttir, S., Bungum, H., Gregersen, S., Havskov, J., Hjelme, H., and Korhonen, H., 1993: Earthquake prediction research in the South Iceland Seismic Zone and the SIL Project. *Bull. Seismol. Soc. Am., 83,* 696-716.

Stefánsson, R., Bonafede, M., Roth, F., Einarsson, P., Árnadóttir, Th., and Gudmundsson, G.B., 2006: *Modelling and parameterizing the Southwest Iceland earthquake release and deformation process.* Vedurstofa Íslands, report VÍ-ES-03, Reykjavík, 50 pp.

Telford, M.W., Geldart, L.P., Sheriff, E.R., and Keys, D.A., 1990: *Applied geophysics* (2nd edition). Cambridge University Press, 860 pp.

Toomey D.R., and Foulger, G.R., 1989: Tomographic inversion of local earthquake data from the Hengill-Grensdalur central volcano complex, Iceland. *J. Geophys. Res., 94-B12,* 17,497-17,510.

Torfason, H., Hersir, G.P., Saemundsson, K., Johnsen, G.V., and Gunnlaugsson, E., 1983: *West Hengill, surface exploration of the geothermal area*. Orkustofnun, Reykjavík, report OS-83119/JHD-22 (in Icelandic), 113 pp.

Tryggvason, K., Huseby, E.S., and Stefánsson, R., 1983: Seismic image of the hypothesized Icelandic hot spot. *Tectonophysics, 100*, 97-118.

Tryggvason, A., Rögnvaldsson, S.Th., and Flóvenz, Ó.G., 2002: Three dimensional imaging of the P- and S-wave velocity structure and earthquake locations beneath Southwest Iceland. *Geophys. J. Int., 151,* 848-866.

Ward, P., and Björnsson, S., 1971: Microearthquakes, swarms and the geothermal areas of Iceland. *J. Geophys. Res., 76,* 953-982.

Weir, N.R.W., White, R.S., Brandsdóttir, B., Einarsson, P., Shimamura, H., Shiobara, H. and the RISE Fieldwork Team, 2001: Crustal structure of the northern Reykjanes Ridge and Reykjanes Peninsula, Southwest Iceland. *J. Geophys. Res., 106,* 6,347-6,368.

APPENDIX I: The temporary seismic networks operated in the Hellisheidi area

STATIONS	SENSOR ID	LATITUDE	LONGITUDE	ELEVATION (m)	STATION NAME
ARRAY 1					
HDT	39033	64N 03.2328	21W 24.9432	262.04	Draugatjarnir
HSM	39046	64N 02.9634	21W 20.0214	530.91	Skarðsmýrarfjall
HSB	39034	64N 03.2592	21W 22.6794	378.79	Sleggjubotnar
HGI	39036	64N 01.4274	21W 22.5036	417.54	Gígir
HHD	39041	64N 01.4748	21W 23.9556	335.4	Hveradalir
HTH	39024	64N 02.2296	21W 22.5444	383.69	Þverfell, high wind
HHH	39023	64N 02.1936	21W 21.0354	395.36	Milli Hrauns og Hlíðar
HHR	39025	64N 02.4636	21W 24.7044	260.13	Hraun
HHU	39035	64N 03.9864	21W 23.0958	416.57	Húsmúli
HID	39051	64N 04.140	21W 19.562	496	Innstidalur, Gps not locked
ARRAY 2					
HMD11	39036	64N 03.1036	21W 17.8773	365	Middalur
HOH12	39033	64N 01.9059	21W 18.1636	381	Orustuholl
HSH13	39025	64N 02.9574	21W 16.1388	403	Svinahlid
HBK14	39024	64N 03.6333	21W 15.4597	383	Brunkollublettir
HBI15	39051	64N 01.9247	21W 16.2686	347	Bitra
HÖH16	39023	64N 03.6399	21W 13.1118	458	Ölkelduhals
HRD17	39034	64N 02.6709	21W 13.2415	382	Reykjadalur
HRB18	39046	64N 01.6071	21W 12.6538	118	Rjupnabrekkur
HGH19	39035	64N 01.1472	21W 25.8754	277	Grauhnjukar

APPENDIX II: Seismic events recorded during June 13 – August 13, 2007

Date	Time	Latitude	Longitude	Depth	No.	Gap	Dist	RMS	ERH	ERZ
07 0616	138 7.88	64 2.02	21 34.07	6.63	31	73	2.5	0.08	0.3	0.4
07 0616	139 25.25	64 2.05	21 34.20	6.76	33	72	2.4	0.08	0.3	0.4
07 0616	148 41.78	64 2.12	21 34.07	6.69	32	72	2.2	0.08	0.3	0.4
07 0616	327 47.25	64 2.28	21 33.71	6.16	30	135	2	0.08	0.3	0.4
07 0616	327 57.67	64 2.00	21 33.52	6.97	17	73	7.3	0.11	0.4	0.8
07 0616	350 21.86	64 1.88	21 33.99	5.14	23	90	2.7	0.08	0.4	0.7
07 0616	652 36.30	64 2.17	21 33.86	6.15	31	71	2.2	0.07	0.3	0.4
07 0616	702 2.49	64 2.21	21 33.53	5.86	21	72	2.2	0.1	0.3	0.4
07 0616	809 54.61	64 2.25	21 33.70	5.8	27	71	2	0.07	0.3	0.4
07 0617	753 39.48	64 1.67	21 33.89	5.61	24	88	3.1	0.1	0.3	0.6
07 0617	1007 18.80	64 2.11	21 34.29	6.13	28	138	2.3	0.07	0.3	0.4
07 0617	1052 53.73	64 4.95	21 34.12	4.38	29	86	3	1.15	2	3.5
07 0617	1343 34.99	64 2.16	21 33.81	5.4	26	71	2.2	0.08	0.3	0.4
07 0619	411 23.23	64 3.15	21 14.40	5.46	41	62	4.6	0.08	0.2	0.3
07 0619	411 23.27	64 3.28	21 14.87	5.37	35	50	4.2	0.12	0.2	0.3
07 0619	2132 49.92	64 6.20	21 17.06	4.55	45	82	6.4	0.08	0.2	0.3
07 0624	1959 38.81	64 3.82	21 13.04	4.81	21	89	5.9	0.09	0.3	0.5
07 0701	2029 27.43	64 6.73	21 16.20	5.68	23	93	7.5	0.09	0.3	0.6
07 0702	2136 12.75	64 3.03	21 14.48	4.97	23	86	5.6	0.08	0.3	0.5
07 0705	353 8.14	64 5.61	21 26.13	5.73	26	61	5.2	0.09	0.2	0.5
07 0706	354 32.90	63 57.14	21 7.74	5.88	28	149	8.5	0.04	0.3	0.7
07 0707	212 31.10	64 4.05	21 16.40	3.65	13	63	8.2	0.05	0.2	0.6
07 0707	212 49.58	64 4.07	21 15.69	4.81	19	70	3.2	0.06	0.3	0.3
07 0707	1006 8.94	63 56.10	21 24.50	6.23	24	132	5.3	0.06	0.2	0.6
07 0709	144 12.95	63 57.77	21 8.14	4.57	39	138	8.4	0.11	0.3	0.8
07 0709	144 14.33	64 1.08	21 20.60	6.39	8	276	1.6	0.08	6.9	12
07 0709	742 17.89	64 1.35	21 35.33	5.66	9	335	8.9	0.03	23.4	4.4
07 0710	1532 12.69	63 56.47	21 26.88	8.26	21	230	7.2	0.1	0.6	0.9
07 0710	1532 12.79	63 56.77	21 26.06	8.12	20	186	6.5	0.06	0.3	0.7
07 0711	1613 27.14	64 4.47	21 17.54	4.9	18	110	1.8	0.04	0.4	0.4
07 0711	1618 41.58	64 4.35	21 17.64	5.14	22	108	1.6	0.04	0.3	0.2
07 0714	428 49.17	64 1.74	21 22.47	2.82	24	59	0.7	0.08	0.2	0.2
07 0714	1021 51.12	64 6.64	21 15.49	6.04	25	96	5.7	0.08	0.3	0.5
07 0714	1021 51.19	64 6.71	21 14.84	5.68	22	101	6.4	0.15	0.5	1.1
07 0715	1009 57.53	64 6.88	21 21.21	4.79	14	152	5.3	0.04	0.5	0.6
07 0716	428 49.16	64 1.74	21 22.65	2.66	27	59	0.7	0.07	0.3	0.2
07 0720	1151 23.66	64 4.33	21 16.09	4.82	14	320	2.9	0.14	1.6	1.7
07 0720	1151 24.80	64 3.08	21 21.97	1.24	20	103	0.7	0.11	0.4	0.2
07 0721	539 3.91	64 3.19	21 13.65	6.02	18	316	5.1	0.04	0.6	1.1
07 0721	539 46.99	64 3.30	21 13.92	6.15	24	196	4.8	0.04	0.3	0.5
07 0721	2301 32.86	64 3.00	21 12.77	6.37	44	66	5.9	0.07	0.3	0.5
07 0723	40 33.69	64 3.34	21 15.15	5.65	29	98	3.9	0.07	0.3	0.6
07 0723	901 57.89	64 3.85	21 23.85	1.3	12	214	0.7	0.06	0.6	0.5
07 0723	1828 18.70	64 2.04	21 33.45	6.98	37	83	2.5	0.07	0.3	0.3

Date	Time	Latitude	Longitude	Depth	No.	Gap	Dist	RMS	ERH	ERZ
07 0724	2141 22.55	64 2.68	21 13.24	5.28	38	67	5.8	0.05	0.3	0.5
07 0724	2142 43.25	64 2.77	21 12.94	5.26	34	67	5.9	0.05	0.3	0.6
07 0724	2144 56.41	64 2.92	21 13.25	5.09	31	72	5.6	0.05	0.3	0.6
07 0724	2144 56.44	64 3.14	21 13.54	5.27	18	316	5.2	0.04	0.5	1.1
07 0725	1254 25.44	64 2.83	21 22.29	0.84	21	57	0.8	0.1	0.2	0.3
07 0725	1312 40.49	64 2.72	21 13.21	5.37	36	67	5.8	0.05	0.3	0.5
07 0728	123 25.52	63 56.37	21 26.49	8.58	30	127	6.8	0.09	0.3	0.5
07 0729	1222 0.93	64 3.06	21 14.24	4.18	37	52	1.1	0.07	0.2	0.2
07 0731	158 50.10	64 3.53	21 11.13	5.29	21	95	2.4	0.04	0.2	0.3
07 0731	727 18.77	64 3.54	21 11.05	5.08	33	74	1.7	0.05	0.2	0.2
07 0801	1247 2.32	64 0.93	21 34.75	6.68	7	345	7.2	0.03	26.2	9.2
07 0801	1247 2.60	64 1.41	21 32.48	6.54	9	338	5.4	0.08	15.8	7.7
07 0805	2035 46.28	63 56.32	21 22.22	4.35	30	133	3.4	0.07	0.2	0.4
07 0806	1408 2.70	64 3.25	21 15.71	4.51	38	49	0.7	0.19	0.4	0.3
07 0807	526 6.63	63 56.65	21 22.15	4.54	30	131	3.2	0.05	0.2	0.5
07 0807	526 6.68	63 56.88	21 22.71	5.67	13	299	8.2	0.05	0.8	2.4
07 0807	1606 27.08	64 5.58	21 17.03	3.78	35	75	3.9	0.08	0.2	0.3
07 0809	1316 22.84	64 1.62	21 34.27	6.77	31	75	3.2	0.07	0.3	0.4
07 0811	726 36.04	64 3.94	21 14.84	4.45	24	96	0.8	0.06	0.2	0.2
07 0811	1331 44.43	64 3.90	21 14.78	4.32	34	94	0.8	0.05	0.2	0.1
07 0811	1339 33.94	64 3.86	21 14.92	4.42	38	95	0.6	0.05	0.2	0.1
07 0811	1341 13.09	64 2.96	21 14.43	4.03	35	52	1.1	0.05	0.2	0.1
07 0811	1354 14.84	64 3.85	21 14.80	4.41	28	94	0.7	0.06	0.2	0.2
07 0813	350 47.91	64 4.13	21 15.26	4.58	31	110	0.9	0.09	0.3	0.2